Properties of Base Neutralized Chitosan-Hydroxyapatite Biocomposite Membrane

Soo-Ling Bee* and Zuratul Ain Abdul Hamid*
School of Materials and Mineral Resources Engineering, Engineering Campus, Universiti Sains Malaysia
Nibong Tebal, 14300 Penang, Malaysia
*Corresponding author (e-mail: sooling0427@gmail.com; srzuratulain@usm.my)

The main objective of this work was to scrutinize the effect of base treatment and hydroxyapatite impregnation on the structural, morphological and antimicrobial properties of the resulting chitosan membranes. In this study, chitosan/hydroxyapatite biocomposite membrane was prepared by solution casting method followed by NaOH treatment for neutralization purpose. It was revealed that the water resistance properties of all composite membrane improved as compared to the pristine chitosan membrane, where their water resistance performance became profoundly augmented as a consequence of NaOH treatment. This is ascribed to the presence of interaction among macromolecular chains or with hydroxyapatite as disclosed by FTIR analysis, which was further supported by the increase in thermal stability as shown by TGA analysis. Incorporation of hydroxyapatite also increase the surface roughness of the resulting membrane, which made them suitable for cell activities. All base-neutralized membranes show no antimicrobial action against *Candida albicans*, thus demonstrating the importance of cationic properties of chitosan in performing its antifungal activity. These preliminary studies can usefully serve as a guideline for future development of chitosan/hydroxyapatite hybrid membrane based on NaOH treatment which have the potential to be used as guided tissue regeneration (GTR) dental membrane for periodontal regeneration application.

Keywords: Chitosan; hydroxyapatite; biocomposites; neutralization; surface property

Received: December 2022; Accepted: April 2023

Chitosan (CS) (1-4)-2-amino-2-deoxy-*β*-D-glucosamine, a partial deacetylated analogue of chitin, is a natural polyaminosaccharide constituting N-acetyl glucosamine and glucosamine units linked by *β*-(1-4)-glycosidic bonds. It is the second most abundant natural biopolymer after cellulose which can be extracted from the exoskeleton of crustaceans, insects, molluscs and cell walls of fungi [1, 2]. Over the years, CS has enticed considerable interest to be fabricated into resorbable membrane for periodontitis treatment due to its intriguing biological properties such as biodegradability, tissue compatibility, wound healing activity and non-toxicity. Furthermore, its structural similarity to the extracellular matrix component of bone, i.e. glycosaminoglycan as well as its non-toxic degraded products that can be easily excreted from the body also made CS a suitable candidate for such application [3, 4]. In addition, CS provides a broad spectrum of antifungal and antibacterial action against numerous microorganisms ascribed to their cationic properties upon dissolution in acidic media [5, 6]. Chitosan also possesses excellent membrane-forming property owning to their ability to form intra- and intermolecular hydrogen bonding [7].

Nevertheless, some limitations including low cellular adhesion and poor resistance to water have become a huge stumbling block for CS membrane to be employed in its application [8]. In recent year, bioactive calcium phosphate such as hydroxyapatite (HA) has been widely utilized in combination with CS in bone tissue engineering due to its compositional and structural similarity to the mineral phase of natural bones [9]. Besides, the addition of HA in CS matrix can be beneficial as it improves the bioactivity property by favouring the protein adsorption and osteoblast attachment on the membrane surface [10]. On top of that, the changes in surface topographic properties and increased in surface roughness of the membrane as a result of filler impregnation can also be a welcomed side effect to further enhance cell adhesion and proliferation [4].

Even though the addition of HA can be useful for improving the bioactivity of the CS membrane, the poor water resistance properties of the CS/HA composite still remain unsolved [8]. In order to make CS/HA composite membrane realizable in clinical practice, various approaches have been taken into consideration to augment the water repellency of CS/HA membrane, such as chemical crosslinking [11-13], radiation crosslinking [14, 15] and post-base treatment [16-19]. Among these methods, base treatment using sodium hydroxide (NaOH) have been extensively employed to enhance the water resistance property due to its facile process without the use of potentially toxic crosslinking agents such as glutaraldehyde [20].

---

†Paper presented at Rubbercon2022

Among the previously reported literatures regarding the employment of base treatment during the post-fabrication of CS-based membrane [21-23], seldom has there been any paper presenting study related to the structural and properties alteration (either been augmented, compensated or deteriorated) of CS membrane as a result of base treatment and HA addition, including the surface topology and antimicrobial properties. Herein, examination of the change in their properties pertaining to the different interaction between CS and HA with emphasis on the influence of filler loading and NaOH treatment will be specifically highlighted in this study.

EXPERIMENTAL SECTION

1.   Materials

CS powder (M_w 50-190 kDa) was purchased from Sigma-Aldrich. Analytical grade glacial acetic acid and sodium hydroxide (NaOH) pellet were obtained from Merck. HA powder was extracted from chicken cortical bone by thermal calcination at 600 ºC according to the previous reported procedure as described in [24]. Throughout the experiment, distilled water was used to prepare aqueous solution. All chemicals were used without further purification.

2.   Preparation of Chitosan/Hydroxyapatite Composite Membranes

The pre-determined amount of HA was dispersed in 10 ml of 1 % acetic acid and sonicated for 3 min to form HA suspension. CS/HA dispersions were prepared by mixing the prepared HA suspension into 1 wt.% of CS solution in 1% acetic acid and mechanically stirred for 1 h. The resulting dispersions were then casted into petri dish and dried in oven at 40 ºC for 48 h to form composite membranes. CS/HA membranes containing different amount of HA (0, 10, 20, 30, 40 and 50 phr) were abbreviated as CS/HA-*x*, where *x* refer to the amount of HA added into the continuous phase. Further to this, the prepared membranes were immersed in 1 mol/L NaOH solution for neutralization, washed with distilled water repeatedly and laminated with glass to prevent the crumpling of membrane. The NaOH-treated films were coded as nCS/HA-*x*.

3.   Characterization Methods

Attenuated Total Reflectance-Fourier Transform Infrared (ATR-FTIR) analysis of the HA, CS and all the composite membranes were determined by a Perkin Elmer Spectrum 100 FTIR spectrometer instrument, USA. All spectra were recorded within the scanning range from 4000 cm^{-1} to 550 cm^{-1}.

Total soluble matter (TSM) of the prepared membrane sample was defined as the percentage of the water soluble dry matter of the membrane after immersion in distilled water. In this study, membranes with 25 x 25 mm dimension were first dried in air-circulating oven for 24 h and accurately weighed as W_i. The dried films were then suspended in 30 ml of distilled water under periodic agitation at ambient condition for 24 h. The non-solubilized film pieces were further filtered and dried (as described above) to determine the remnant weight (W_f) of the dry matter. TSM was calculated based on the following equation [25]:

$$TSM\ (\%) = \frac{W_i - W_f}{W_i} \times 100 \qquad (1)$$

Three replicates were performed for each formulation.

The thermal stability of the HA, CS and all their composites were evaluated by thermogravimetric analysis (PerkinElmer Pyris 6 TGA, USA) at a scanning range from 30 ºC to 600 ºC at a constant heating rate of 10 ºC/min under nitrogen atmosphere.

The surface topography and morphology of the composite membranes were investigated by atomic force microscope (AFM) (Bruker, Multimode 8, USA). The scanning area for images was set at 5 x 5 µm^2.

Antimicrobial activities of all the CS samples were studied against the growth of *Candida albican* using the Kirby-Bauer agar diffusion method. Herein, *Candida albican* was chosen for antimicrobial testing as it is one of the common oral pathogen present in the oral cavity. Briefly, the tested bacteria was inoculated by mixing a few colonies of bacteria from exponential growth phase in 5 ml of sterilized nutrient broth and incubated at 37 ºC for 24 h. Before subjecting the culture to test, the bacterial suspension was diluted using saline, vortexed and compared with the standard McFarland solution (0.5%, 10^6 -10^8 CFU/ml) to ensure the cell concentration was approximately at 1×10^6 CFU/ml. Then, the tested bacteria were spread uniformly throughout the entire surfaces of solidified Mueller Hilton agar plates using sterile cotton swaps and the samples were placed onto the agar plates. The plates were incubated at 37 $\pm$ 2 ºC for 24 h and the zone of inhibition was measured.

RESULTS AND DISCUSSION

1.   Total Soluble Matter (TSM)

In this study, TSM is used to indicate the resistance of the prepared CS membrane towards water washout. Fig. 1(a) shows the TSM of all the prepared CS-based membranes after immersing in water for 24 h. As can be seen, the solubility of the CS membrane decreases upon the addition of HA. The relatively higher TSM exhibited by pristine CS/HA-0 membrane could be related to the presence of acetate ions that electro-statically bound to the protonated amine groups in CS matrix, thus disrupting their latter inter- and intra-molecular hydrogen bonds as illustrated in Fig. 2(a).
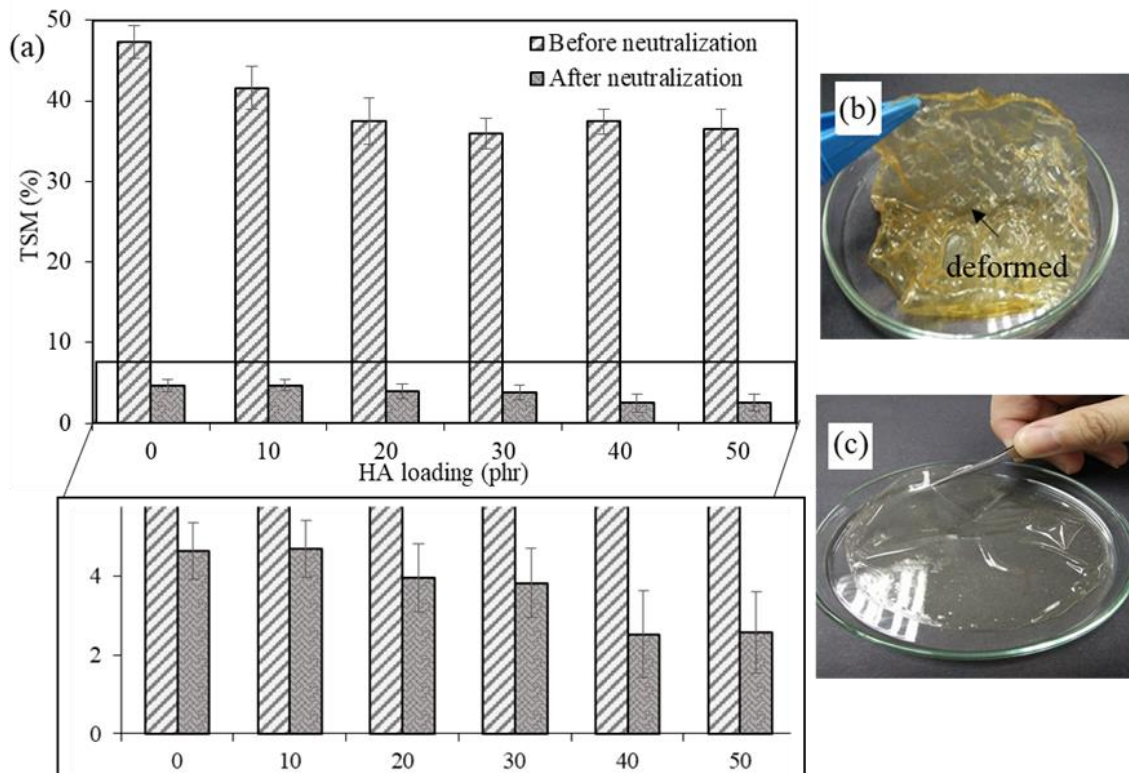
Figure 1. (a) TSM of the CS-based membranes prior to and after base neutralization, image of the (b) as-casted CS/HA-0 and (c) NaOH-neutralized nCS/HA-0 membranes after immersed in water.

Hence, the macromolecular chains tend to be desorbed and solubilized when agitated in water. Meanwhile, the decrement of TSM upon the addition of HA is likely to be caused by the hydrogen and electrostatic interaction between the hydroxyl and phosphate domain of HA with the hydrophilic region of CS chain (using their NH_3^+ and OH groups) (Fig. 2 (b)) that make their polar groups become less accessible to water molecules, thereby slightly hinder the polymer desorption in aqueous medium.

On the other hand, water resistance property of the CS-based membrane improves remarkably after NaOH treatment. The decrease of soluble matter in NaOH-treated film can be related to the reduction of the protonated amino groups after neutralization as shown in the following equation. (--- indicates the electrostatic interaction)

Meanwhile, except for nCS/HA-10 sample, all NaOH-treated composite membranes shown slightly lower TSM as compared to pure NaOH-treated CS membrane. This is due to the increased hydrogen bonding interaction between CS chains and HA which tends to reduce the availability of polar moieties for subsequent interactions with water molecules. In addition, the regenerated amine groups can also act as electron pair donor to be covalently bonded to the Ca^{2+} from HA via coordination bonding as illustrated in Fig. 2(d), thus further stabilizing the integrity of the CS network [21].

It is important to highlight that the decrement of TSM in CS membrane after NaOH treatment is significantly more drastic compared to that of CS membrane after the addition of HA. This is due to the formation of intermolecular hydrogen bonding between

$$CS\text{-}NH_3^+\text{---}^-OOCCH_3 + NaOH \rightarrow CS\text{-}NH_2 + CH_3COO^-Na^+ + H_2O \qquad (2)$$

Deprotonation of amino groups will strengthen the intra- (via HO3---O5 hydrogen bond) and inter-chains interaction (Fig. 2(c)), thus improving the CS macromolecules stability and decreasing their solubility [26]. Moreover, NaOH treatment also remove the remnant acetic acid from the CS matrix to hinder further dissolution when in contact with water. Fig. 1(b) and (c) demonstrated the impact of as-casted and NaOH-treated CS membrane after immersing in water.

CS chains to form a stronger polymer network that will be more effective in preserving the stability and integrity of CS membrane when suspended and agitated in water. On the other hand, the interaction between HA and CS solely is insufficient to maintain the overall membrane stability in water (even though the TSM value decrease slightly after the addition of HA) due to the less amount of HA involved in securing the CS chains together. This is attributed to the competition

between the phosphate groups (from HA) and acetate groups (from acetic acid) to interact with $-NH_3^+$ groups from CS chains. Fig. 3 illustrates the comparison of

NaOH treatment and HA addition on the structural stability and solubility aspect of CS membrane when suspended in water.
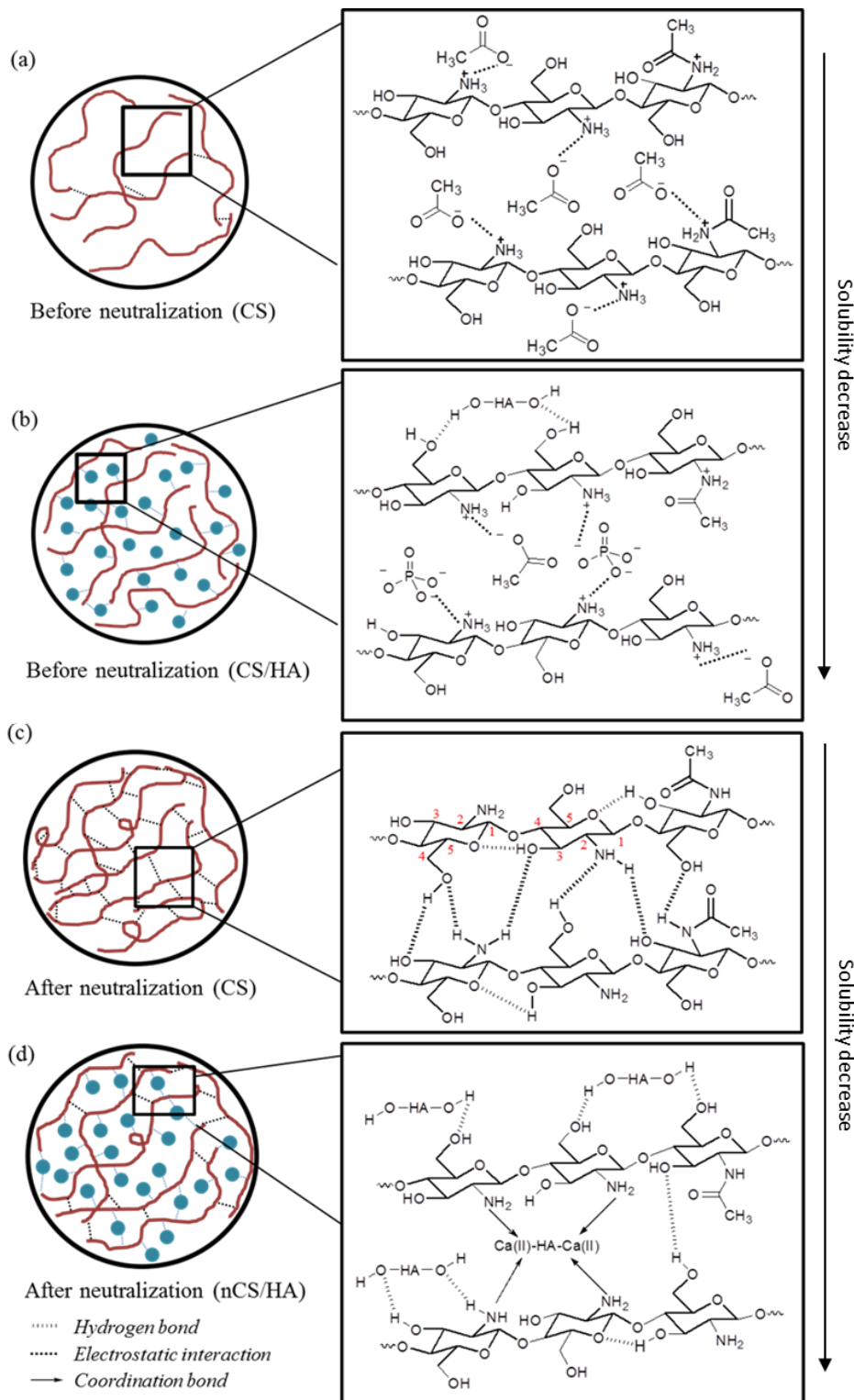

Figure 2. Schematic illustration depicting the possible interaction within the macromolecular matrices.
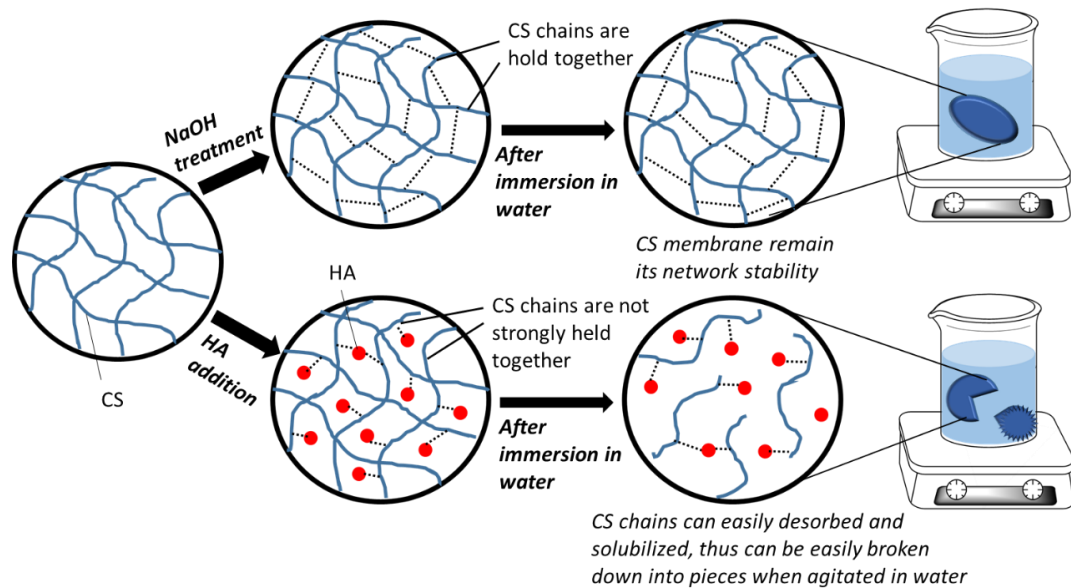
Figure 3. Schematic illustration comparing the impact of NaOH treatment and HA addition on the structural stability and solubility aspect of CS membranes when suspended and agitated in water.

2.   FTIR Analysis

FTIR analysis was employed to ascertain the presence of possible interactions as well as change in chemical functionalities of CS membrane as a result of base neutralization and HA impregnation. As depicted in Fig. 4, the pristine CS/HA-0 film displayed a broad peak at 3000-3500 cm^{-1} due to the overlapping of N-H and O-H stretching vibration. The peaks observed at 2922 and 2822 cm^{-1} can be assigned to the symmetric and asymmetric C-H vibrations. The characteristics bands attributable to the amide I (C=O stretching) and amide II (N-H bending) were also found in 1632 and 1543 cm^{-1}, respectively. Notably, these peaks were in slightly lower wavenumber when compared with undissolved CS powder (1634 and 1592 and cm^{-1}) due to the protonation of amine groups by acetic acid [8]. The presence of band at 1406 cm^{-1} is ascribed to the symmetric stretching of carboxylate ions (COO^{-}) which is responsible for breaking the intermolecular bonding between CS chains [19]. Other peaks corresponding to the pyranose rings such as asymmetrical stretching of C-O-C glycosidic bridge (1151 cm^{-1}) and skeletal C-O stretching (1067 and 1023 cm^{-1}) were also observed in FTIR spectrum [27].

As compared to the pure CS/HA-0 film, the intensities of the peaks that are corresponding to the amide I and II decreased significantly after NaOH treatment. This is due to the decrease amount of protonated amine group engendering from base neutralization that devitalizes their hydration shielding effect [26]. Moreover, these peaks also slightly shifted toward higher wavenumbers value after NaOH treatment. This results could be due to the formation of intermolecular hydrogen bonding between the -NH$_2$ and -OH moieties between the CS polymer chains. This result explains the resistance of the CS membrane toward water washout after NaOH treatment. On the other hand, the bands assigned to CH$_2$ bending vibration mode which was previously overlapped with the carboxylate peak reappear after base treatment [19]. It is worthwhile to mention that the base-neutralized sample depicts the same peaks as CS powder evidencing the removal of acetate groups from the polymer matrix.

Incorporation of HA into the CS matrix also shift the characteristics peak of N-H bending toward slightly higher values. Furthermore, the intensity of the O-H band also reduced considerably after HA impregnation. All this results suggest the possible hydrogen-bonding interaction between the abundant NH$_2$ and OH groups from the CS chains with OH groups from the HA as well as coordination bonding between regenerated NH$_2$ groups with Ca^{2+} as suggested previously [9, 21]. For untreated film, the decrement of N-H peaks intensity upon HA addition (> 20 phr loading) can also be attributed to the existence of possible electrostatic interaction and hydrogen bonding between -NH$_3^{+}$ of CS and PO$_4^{3-}$/OH groups of HA.
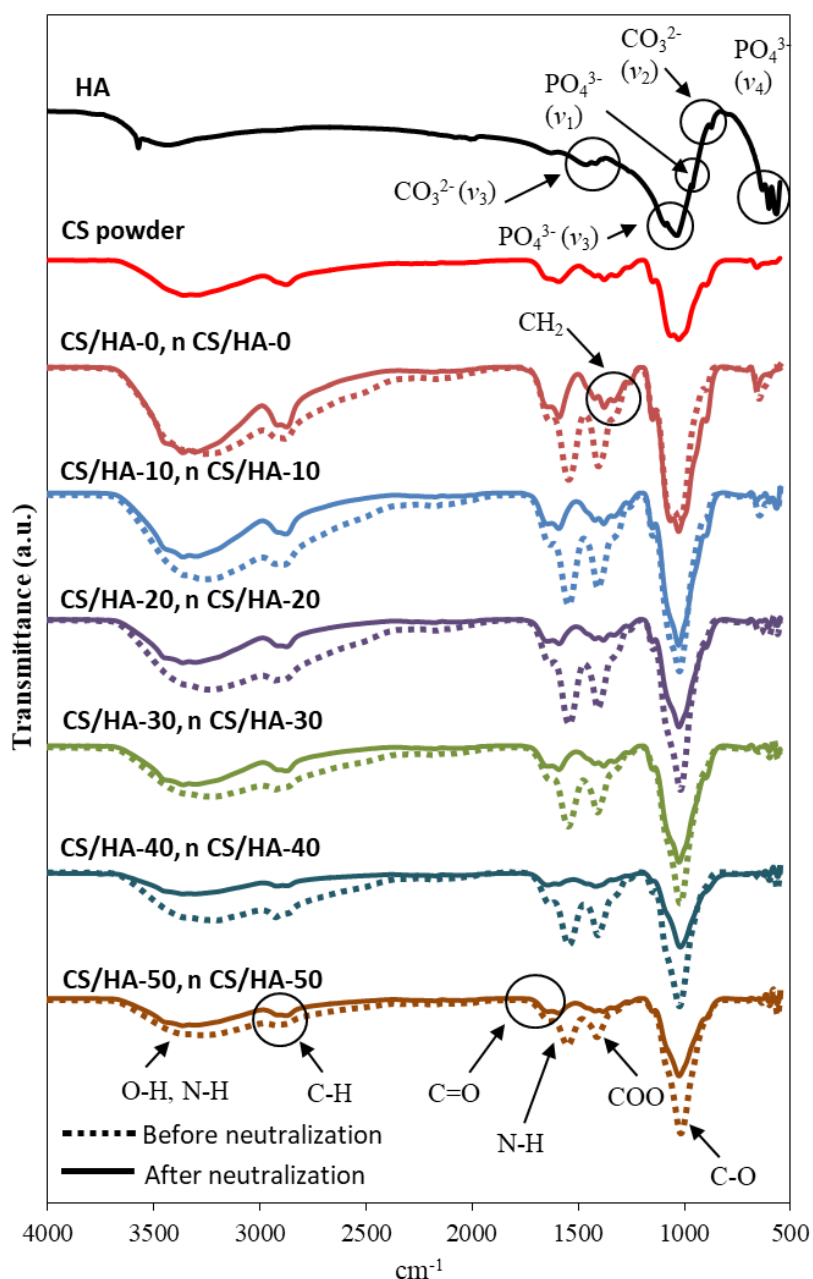
Figure 4. FTIR-ATR spectra of HA, CS powder and all CS membrane with varying HA formulation prior to and after NaOH treatment.

3.   Thermal Study

Thermal stability of HA, CS and their composite membranes with different filler loadings prior to and after NaOH treatment were studied by TGA as shown in Fig. 5. Basically, HA does not show any thermal decomposition up to 600 °C, which confirm the absence of any organic phase (such as collagen or other protein) in the HA used in this research. From the fundamental point of view, thermal behavior of the fabricated membrane can be useful as it reflects the supramolecular organization of CS by accessing their thermal stability at different formulation. It can work together with FTIR to further understand the possible interaction between CS and the HA particles that can be involved

as a result of base neutralization. Generally, pure CS/HA-0 and nCS/HA-0 samples exhibit two thermal degradation event. The first step of thermal decomposition below 160 °C is ascribed to the evaporation of physically weak and chemically strong bound moisture and residual solvent (such as acetic acid) from the samples. It is noticed that as-casted film shown higher moisture content compared to alkaline-treating film due to their protonated amino group that have greater affinity toward water molecules [28]. Furthermore, formation of intermolecular hydrogen bonding between CS chains may reduce the subsequent interaction of CS with water molecules [29]. Likewise, the reduction of moisture content with increasing HA concentration also substantial the possible interaction

between HA and CS as previously discussed in FTIR. On the other hand, the subsequent weight loss observed between 160 °C and 400 °C is attributed to the decomposition of the acetylated and deacetylated units, depolymerization and destruction of pyranose ring of CS structure [4, 30, 31]. Compared to the un-neutralized sample, base treatment appears to have positive impact in improving the thermal stability of the CS film. This is attributed to the increased hydrogen interaction between adjacent CS chains that require higher energy to degrade the CS structure.

In both un-neutralized and neutralized samples, similar degradation trends were observed for all the HA-loaded composites counterpart, where their decomposition begin at a slightly higher temperature, thus indicating a better thermal stability upon HA addition. This can be explained by the hydrogen bonding between the CS chains and HA that allow a better heat dissipation over several bonds. In addition, increasing in the amount of HA loading tends to improve the thermal degradation of the resulting composite samples (in both un-neutralized and neutralized samples) due to the more interaction that existed between CS chains and HA filler. The higher char residue in comparison to the pristine sample indicates the presence of inorganic phase in CS membrane.
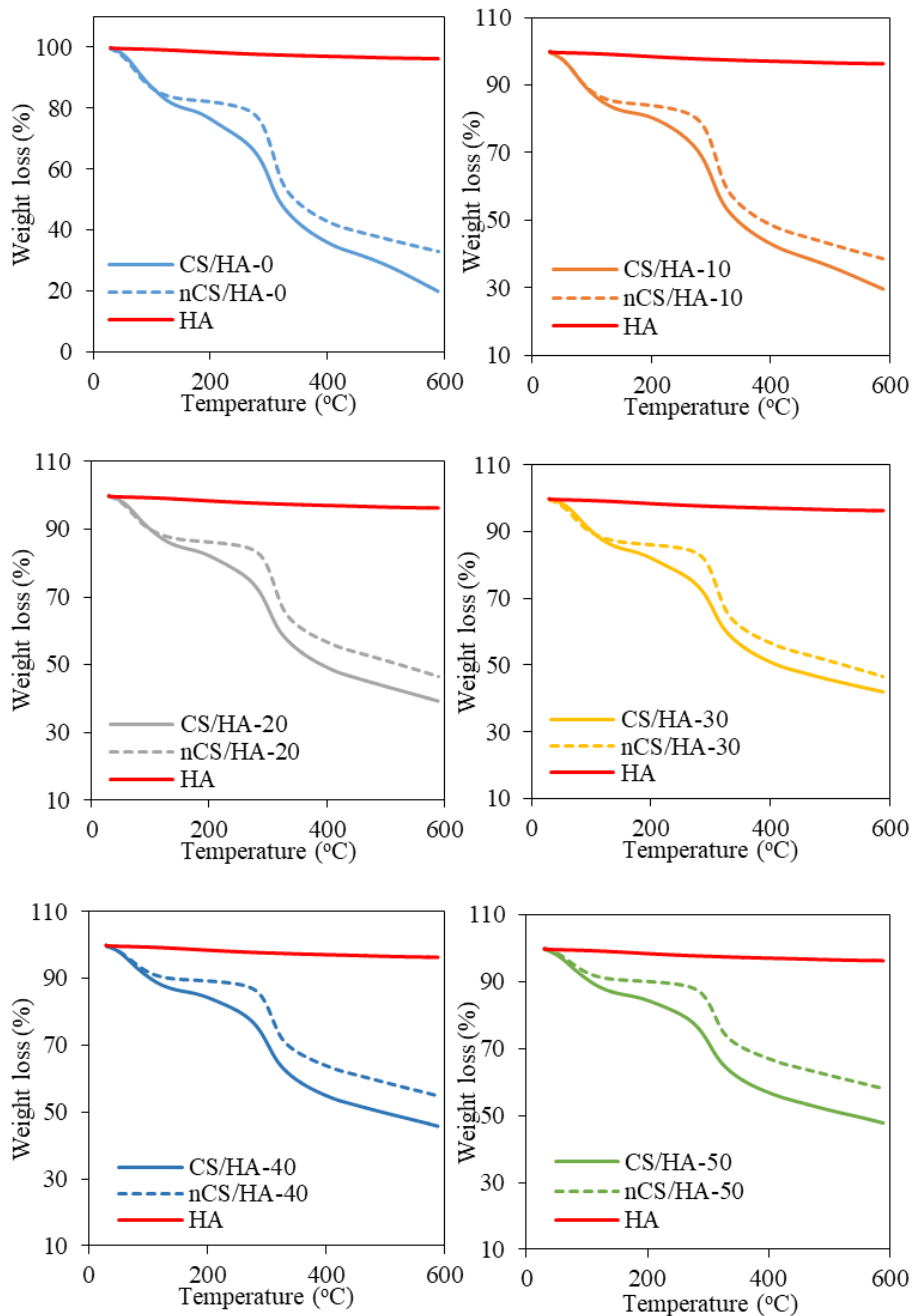

Figure 5. TGA thermograms of the as-casted and base neutralized CS film with varying HA loading.
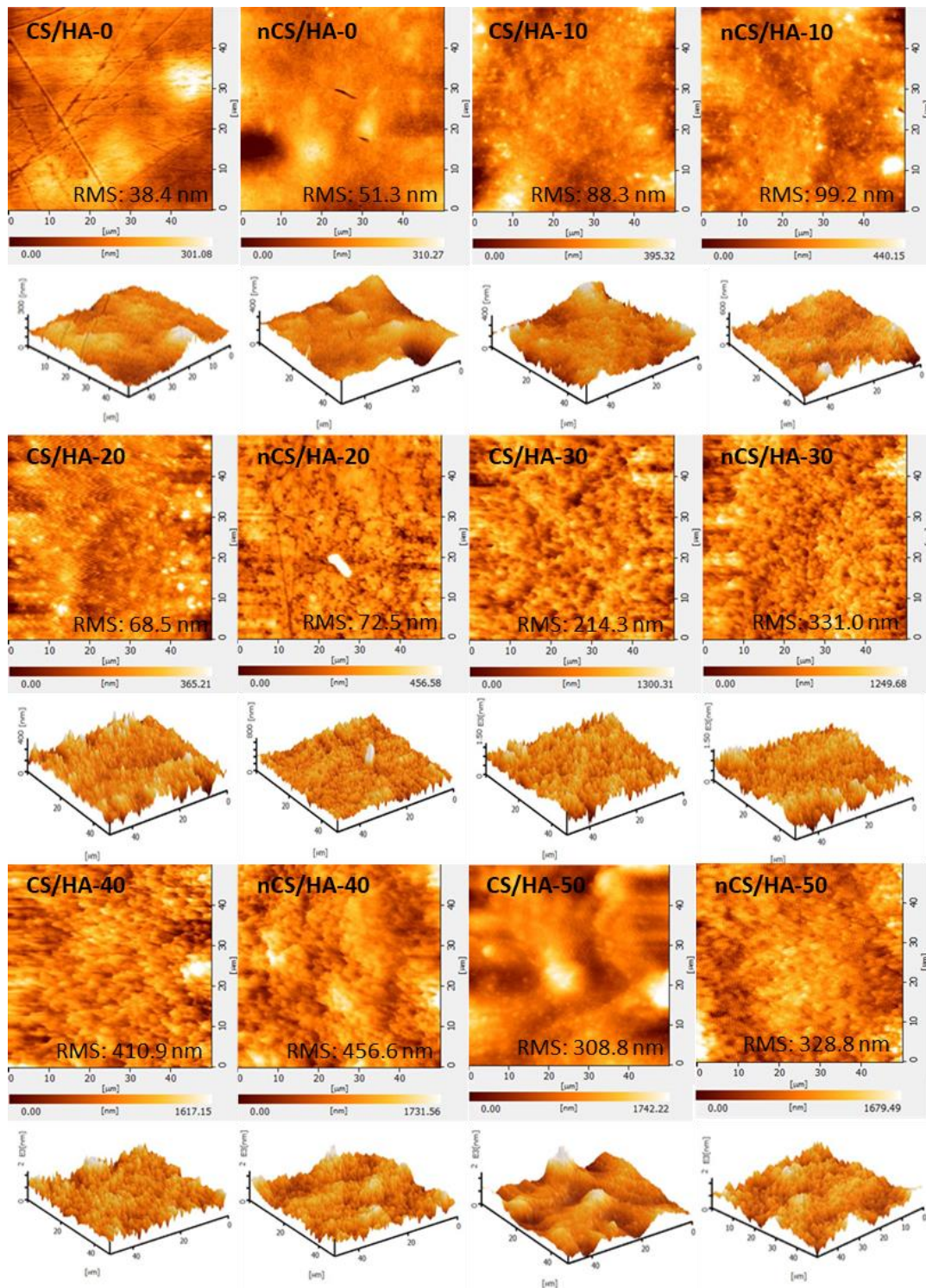
Figure 6. 2D, 3D topographic AFM images and RMS values of all prepared membranes.

4.   Surface Property

Surface characteristics such as topography and roughness of the membrane are important aspects for periodontal regeneration as it significantly influences the initial protein adsorption and cell behaviour after implantation. As can be seen in Fig. 6, pristine CS membrane is relatively smooth, showing only few topographic features that is ascribed to the sample preparation procedure, where its root mean square roughness

(RMS) was determined about 38.4 nm. For composite membranes, their surface morphology is relying on the amount of filler added. The membrane prepared with low loading of HA presents some small protruding structure on the surface, which upon HA content >20 phr reveal relatively coarse topography with more concentrated protuberance on the surfaces. This is evidenced by the drastic increase of RMS values observed for high loading composite membrane. It seems incorporation of HA particles into CS matrix

leads to aggregation and inhomogeneity due to the high surface energy of HA, and thus forming bumpy structure on the surface of composites after solvent evaporation [32]. These rough surfaces induced by high HA impregnation is prominent for supporting protein adsorption and cell activities such as cell attachment and proliferation on biomaterial surface [4].

On the other hand, the slight increase in RMS value of the base-neutralized membrane, specifically for high loading composites suggesting the vague increase in surface roughness after NaOH neutralization. This might be due to the contraction of CS matrix as a result of their inter-hydrogen interaction.

5.   Antimicrobial Study

For the purpose of assessing whether the addition of HA and base treatment can affect the antifungal property of the resulting CS membrane, their inhibitory effect against oral pathogen i.e. *Candida albicans* were studies. As mentioned in previous literature [33], the antimicrobial activity of the CS is related to the interaction between its cationic amine groups with the negatively charge microbial membrane that will alter the membrane permeability. This will lead to the subsequent leakage of proteinaceous and intracellular components, which eventually causing cell death. Table 1 presents the antimicrobial efficacies of all the composite samples as a function of increasing HA loading and base treatment. For all the un-treated samples, it can be observed that the antifungal activity of the CS decreases slightly upon the addition of HA. This can be attributed to the interaction between HA and the cationic $-NH_3^+$ groups of CS that hinder the subsequent action of these cationic $-NH_3^+$ groups of CS to interact with the negatively charge microbial membrane to carry out the antimicrobial action. On the other hand, all the base-treated CS membranes do not show any antimicrobial action against *Candida albicans*. This could be attributed to the loss of their poly-

cationic properties during neutralization process, as corroborated by FTIR. This result showed that although NaOH treatment can be effective in offering the water resistance properties for CS membrane to fulfil the basic requirement for its application, the loss of their antimicrobial properties seem to be an unavoidable aspect that required to be taken into consideration during the designation of CS-based materials.

CONCLUSIONS

In this study, CS/HA biocomposite membranes prepared by solution casting approach were studied pertaining to their structural-properties relationship as a function of increasing HA content and base treatment. According to the results obtained from FTIR and TGA analysis, it is suggested that there is possible weak interaction (electrostatic and hydrogen interaction) between HA and CS matrix in all untreated composite membranes, while base deprotonation of membrane result in the formation of inter- and intramolecular hydrogen interaction among macromolecular chains as well as coordinate bonding between regenerated amine groups of CS with calcium ions from HA. It is worthwhile to mention that the abovementioned interactions are responsible for the enhancement in water resistance properties of CS membrane as a consequences of filler addition and base neutralization. Meanwhile, the surface morphology of membrane is significantly affected by the HA content, where the surface roughness of the membrane increases with the rises of HA concentration. The loss of polycationic properties of CS membranes as a consequence of base deprotonation also resulted in the loss of antifungal properties of CS. This outcome significantly demonstrates the shortcoming of base neutralization that will diminish the antifungal property of CS despite its effectiveness to improve the water resistance property of the membrane. Hence, further research that focus on optimizing the properties of CS/HA biocomposite membrane (such as inclusion of antimicrobial agent) will be the subject in our future research.

Table 1. Antifungal activity of all samples against *Candida albicans* expressed in terms of diameter of inhibition zone.

Samples	Diameter of inhibition zone (mm)
CS/HA-0	4.5
CS/HA-10	4.2
CS/HA-20	4.4
CS/HA-30	4.2
CS/HA-40	4.1
CS/HA-50	4.0
nCS/HA-0	-
nCS/HA-10	-
nCS/HA-20	-
nCS/HA-30	-
nCS/HA-40	-
nCS/HA-50	-

REFERENCES

1. Ahmed, S., Ikram, S. (2016) Chitosan based scaffolds and their applications in wound healing. *Achiev. Life Sci.*, **10**, 27-37.

2. Anitha, A., Sowmya, S., Kumar, P. S., Deepthi, S., Chennazhi, K. P., Ehrlich, H., Tsurkan, M., Jayakumar, R. (2014) Chitin and chitosan in selected biomedical applications. *Prog. Polym. Sci.*, **39**, 1644-1667.

3. Onishi, H., Machida, Y. (1999) Biodegradation and distribution of water-soluble chitosan in mice. *Biomaterials*, **20**, 175-182.

4. Tamburaci, S., Tihminlioglu, F. (2018) Novel poss reinforced chitosan composite membranes for guided bone tissue regeneration. *J. Mater. Sci. Mater. Med.*, **29**, 1-14.

5. Hosseinnejad, M., Jafari, S. M. (2016) Evaluation of different factors affecting antimicrobial properties of chitosan. *Int. J. Biol. Macromol.*, **85**, 467-475.

6. Hamedi, H., Moradi. S., Hudson, S. M., Tonelli, A. E. (2018) Chitosan Based Hydrogels and Their Applications for Drug Delivery in Wound Dressings: A Review. *Carbohydr. Polym.*, **199**, 445-460.

7. Ma, Y., Xin. L., Tan, H., Fan, M., Li, J., Jia, Y., Ling, Z., Chen, Y., Hu, X. (2017) Chitosan membrane dressings toughened by glycerol to load antibacterial drugs for wound healing. *Mater. Sci. Eng. C.*, **81**, 522-531.

8. Fernandez-de Castro, L., Mengíbar, M., Sánchez, Á., Arroyo, L., Villarán, M. C., de Apodaca, E. D., Heras, Á. (2016) Films of chitosan and chitosan-oligosaccharide neutralized and thermally treated: Effects on its antibacterial and other activities. *LWT-Food Sci. Technol.*, **73**, 368-374.

9. Nazeer, M. A., Yilgör, E., Yilgör, I. (2017) Intercalated chitosan/hydroxyapatite nanocomposites: promising materials for bone tissue engineering applications. *Carbohydr. polym.*, **175**, 38-46.

10. Li, X., Nan, K., Shi, S., Chen, H. (2012) Preparation and characterization of nano-hydroxyapatite/

chitosan cross-linking composite membrane intended for tissue engineering. *Int. J. Biol. Macromol.*, **50**, 43-49.

11. Yu, Q., Song, Y., Shi, X., Xu, C., Bin, Y. (2011) Preparation and properties of chitosan derivative/ poly (vinyl alcohol) blend film crosslinked with glutaraldehyde. *Carbohydr. Polym.*, **84**, 465-470.

12. Liang, J., Wang, R., Chen, R. (2019) The impact of cross-linking mode on the physical and anti-microbial properties of a chitosan/bacterial cellulose composite. *Polymers*, **11**, 491.

13. Zhuang, L., Zhi, X., Du, B., Yuan, S. (2020) Preparation of elastic and antibacterial chitosan–citric membranes with high oxygen barrier ability by in situ cross-linking. *ACS omega*, **5**, 1086-1097.

14. Shahbazi, M., Rajabzadeh, G., Ahmadi, S. J. (2017) Characterization of nanocomposite film based on chitosan intercalated in clay platelets by electron beam irradiation. *Carbohydr. polym.*, **157**, 226-235.

15. Zhang, D., Yang, S., Chen, Y., Liu, S., Zhao, H., Gu, J. (2018) 60Co γ-ray irradiation crosslinking of chitosan/graphene oxide composite film: Swelling, thermal stability, mechanical, and anti-bacterial properties. *Polymers*, **10**, 294.

16. Corsello, F. A., Bolla, P. A., Anbinder, P. S., Serradell, M. A., Amalvy, J. I., Peruzzo, P. J. (2017) Morphology and properties of neutralized chitosan-cellulose nanocrystals biocomposite films. *Carbohydr. Polym.*, **156**, 452-459.

17. Mota, J., Yu. N., Caridade, S. G., Luz, G. M., Gomes, M. E., Reis, R. L., Jansen, J. A., Walboomers, X. F., Mano, J. F. (2012) Chitosan/ bioactive glass nanoparticle composite membranes for periodontal regeneration. *Acta biomater.*, **8**, 4173-4180.

18. Rubentheren, V., Ward, T. A., Chee, C. Y., Nair, P. (2015) Physical and chemical reinforcement of chitosan film using nanocrystalline cellulose and tannic acid. *Cellulose*, **22**, 2529-2541.

19. Noriega, S. E.; Subramanian, A. (2011) Consequences of neutralization on the proliferation and cytoskeletal organization of chondrocytes on chitosan-based matrices. *Int. J. Carbohydr. Chem.*, **2011**, 809743.

20. Zhang, D., Zhou, W., Wei, B., Wang, X., Tang, R., Nie, J., Wang, J. (2015) Carboxyl-modified poly (vinyl alcohol)-crosslinked chitosan hydrogel films for potential wound dressing. *Carbohydr. polym.*, **125**, 189-199.

21. Xianmiao, C., Yubao, L., Yi, Z., Li, Z., Jidong, L., Huanan, W. (2009) Properties and in vitro

biological evaluation of nano-hydroxyapatite/ chitosan membranes for bone guided regeneration. *Mater. Sci. Eng. C*, **29**, 29-35.

22. Fraga, A. F., de Almeida Filho, E., da Silva Rigo, E. C.; Boschi, A. O. (2011) Synthesis of chitosan/ hydroxyapatite membranes coated with hydroxy-carbonate apatite for guided tissue regeneration purposes. *Appl. Surf. Sci.*, **257**, 3888-3892.

23. Zhang, K., Zhao, M., Cai, L., Wang, Z. K., Sun, Y. F., Hu. Q. L. (2010) Preparation of chitosan/ hydroxyapatite guided membrane used for periodontal tissue regeneration. *Chinese J. Polym. Sci.*, **28**, 555-561.

24. Bee, S. L., Hamid, Z. A. A. (2019) Characterization of chicken bone waste-derived hydroxyapatite and its functionality on chitosan membrane for guided bone regeneration. *Composites Part B: Engineering.*, **163**, 562-573.

25. Davoudi, Z., Rabiee, M., Houshmand, B., Eslahi, N., Khoshroo, K., Rasoulianboroujeni, M., Tahriri, M., Tayebi, L. (2018) Development of chitosan/ gelatin/keratin composite containing hydrocortisone sodium succinate as a buccal mucoadhesive patch to treat desquamative gingivitis. *Drug Dev. Ind. Pharm.*, **44**, 40-55.

26. Takara, E. A., Marchese, J., Ochoa, N. A. (2015) NaOH treatment of chitosan films: Impact on macromolecular structure and film properties. *Carbohydr. polym.*, **132**, 25-30.

27. Liu, J., Liu, S., Wu, Q., Gu, Y., Kan, J., Jin, C. (2017) Effect of protocatechuic acid incorporation on the physical, mechanical, structural and anti-oxidant properties of chitosan film. *Food Hydrocoll*, **73**, 90-100.

28. Gartner, C., López, B. L., Sierra, L., Graf, R., Spiess, H. W., Gaborieau, M. (2011) Interplay between structure and dynamics in chitosan films investigated with solid-state NMR, dynamic mechanical analysis, and X-ray diffraction. *Biomacromolecules*, **12**, 1380-1386.

29. Kadam, D., Shah, N., Palamthodi, S., Lele, S. S. (2018) An investigation on the effect of poly-phenolic extracts of Nigella sativa seedcake on physicochemical properties of chitosan-based films. *Carbohydr. polym.*, **192**, 347-355.

30. Vilela, C., Pinto, R. J., Coelho, J., Domingues, M. R., Daina, S., Sadocco, P., Santos, S. A., Freire, C. S. (2017) Bioactive chitosan/ellagic acid films with UV-light protection for active food packaging. *Food hydrocoll.*, **73**, 120-128.

31. Tan, W., Li, Q., Dong, F., Zhang, J., Luan, F., Wei, L., Chen, Y., Guo, Z. (2018) Novel cationic chitosan derivative bearing 1, 2, 3-triazolium and pyridinium: Synthesis, characterization, and anti-fungal property. *Carbohydr. polym.*, **182**, 180-187.

32. Nikpour, M. R., Rabiee, S. M., Jahanshahi, M. (2012) Synthesis and characterization of hydro-xyapatite/chitosan nanocomposite materials for medical engineering applications. *Compos B Eng.*, **43**, 1881-1886.

33. Tayel, A. A., Moussa, S., Wael, F., Knittel, D., Opwis, K., Schollmeyer, E. (2010) Anticandidal action of fungal chitosan against Candida albicans. *Int. J. Biol. Macromol.*, **47**, 454-457.